International Journal of Scientific & Engineering Research, Volume 8, Issue 6, June-2017
ISSN 2229-5518

Modelling of Tsunami Intensity Using Artificial Neural Network and Fuzzy Inference Systems

M.A.N. Dewapriya, W.P.S. Dias, T.G.S. Peiris

Abstract—A database compiled by V. K. Gusiakov was used to model tsunami intensity using various other parameters (i.e. earthquake moment magnitude, focal depth, tsunami efficiency, and distance to the nearest shore) as explanatory variables. For the modelling, artificial neural networks, adaptive network based fuzzy inference systems, and multiple linear regression techniques were employed. The modelling is used not so much for mathematical representation, but to explore the current knowledge about physical parameters related to tsunamis. We show that transforming the tsunami intensity values I to 2^I yields better correlations. Earthquake moment magnitude values greater than 8 cause substantial tsunamis, and the effects of the other explanatory variables are not very significant. There is a large scatter of tsunami intensity versus earthquake moment magnitude, justifying a two-valued prediction scheme, but this scatter reduces substantially with the increase of earthquake moment magnitude. The performance of artificial neural networks is better when compared with the other two modelling schemes; however, the changes in membership functions of the fuzzy inference system give us some genuine domain knowledge.

Index Terms— earthquake magnitude, tsunami intensity, fuzzy inference systems, neural networks, multiple regressions.

1 Introduction

VARIOUS relationships have been proposed between tsunami intensity (I) and earthquake magnitude (Mw) [1], [2], [3]. In most of these, earthquake magnitude alone has been used to predict tsunami intensity and no indication has been given regarding the variability of the relationships. Chubarov and Gusiakov [2] propose a linear relationship between I and Mw, whereas Blackford [3] proposes a linear relationship between $\log_{10}$ Hav and Mw, where Hav is the average wave height in metres along the nearest coast to the earthquake location.

Researchers have also studied other factors that could influence tsunami intensity, while acknowledging that Mw is the dominant influence on I. Okal [4] used numerical simulations to deduce that focal depth (up to 100-150 km) and slip direction were less important factors than the orientation of the fault plane to the target coast and the variation of ocean depth perpendicular to the path of the tsunami wave. Geist et al. argue that higher water depths cause greater tsunami wave heights in the near field [5], [6]; this effect has been noted for far field tsunamis too [4]. Geist [5] also quotes Abe [7], who argues that the relationship between Hav and Mw would be different for near and far field tsunamis, suggesting that distance to the source could be a parameter of significance.

Gica et al. [8] used a numerical model to examine the effect of different earthquake fault plane parameters (dip, strike and rake angles, fault dimensions, slip displacement and focal depth) on tsunami wave height in the far field. The wave height was found to increase with a decrease in focal depth from 93 to 33 km, justifying the argument that if an earthquake happens closer to the earth surface, it would cause a stronger disturbance and generate a higher tsunami wave; this effect was reversed however at focal depths below 33 km and also not noticeable for very distant earthquakes. Other fault plane parameters were found to have varying significance [8], [9].

For various regions in the Pacific, Gusiakov [10] determined a quantitative value called the Tsunami Efficiency (TE) coefficient. The coefficient TE is calculated as the percentage ratio between the number of tsunamis of tectonic, landslide, and unknown origin and the total number of coastal and submarine earthquakes with surface magnitude greater than 7.0 and depth less than 100 km that occurred within a given region during time period from 1901 to 2000. Based on the TE for each tsunamigenic region, Gusiakov [10] divided the regions into three categories, named Red (TE is above 60%), Green (TE between 40–60%) and Blue (TE less than 40%), that roughly correspond to the increased, normal and decreased levels of this ratio as compared to the average for the whole Pacific. He then used a numerical model to generate tsunami intensities from earthquakes in the Pacific during 1900-1998. A plot between earthquake magnitude (Mw) and resulting tsunami intensity on the Soloviev-Imamura scale (I) showed that earthquakes in the red region generate tsunamis with higher intensity than those in the other two regions [11].

The main objectives of this study are to model the likelihood and intensity of tsunamis for recorded earthquake magnitudes and other relevant parameters, and to evaluate the comparative advantages of input-output modelling schemes such as artificial neural networks (ANN), adaptive network based fuzzy inference systems (ANFIS), and multiple regression (MR). The main independent variable is the earthquake moment magnitude, Mw [12], while the dependent variable is tsunami intensity, I, defined [2] as

• *This work is based on resrarch carried out for a master's research degree at the University of Moratuwa, Sri Lanka by the first author on a research grant from the Senate Research Committee, under the supervision of the second author, with assistance from the third author.*

$$I = \tfrac{1}{2} + \log_2 Hav \quad (1)$$

This tsunami intensity is also known as the Soloviev-Imamura scale [13] (quoted by Gusiakov in [14]). It must be noted that using a single measure such as tsunami intensity could mask the great many variations inherent in a phenomenon such as a tsunami [15]. However, it would be sufficient for the level of accuracy desired in this research. This is because the main purpose of the modelling was not the derivation of precise mathematical relationships, but rather the exploration of current knowledge regarding physical parameters related to tsunamis.

There are two ways in which this paper seeks to make a specific contribution to the existing knowledge. The first is that it seeks to use recorded historical data rather than generated data (used by many other researchers). The second is that it has focused on parameters that can be used immediately after an earthquake so that the model could be used in a predictive mode, thus contributing to a decision as to whether a tsunami warning should be issued or not. So, very specific source data such as slip direction and fault dimensions are not used. However, inputs such as distance to the source and focal depth are explored, in addition to Mw, the dominant factor. While technology is available for real time computing and data driven models [16], there is also arguably a role for greater robustness in simple models, in order to serve as checks on the more sophisticated models, and to make quick computations in the field.

In this work, three modelling techniques (i.e. ANN, ANFIS, and MR) were employed to derive the relationships between Mw and I. MR is a classical way of finding relationships among different variables. Meanwhile, though lacking the formality of regression techniques, ANNs have become a powerful way of establishing input-output relationships. Various approaches have been used to minimize the black box nature of ANNs, including the use of sensitivity analysis. ANFIS is a newly emerging alternative to ANNs, where some rationality regarding the model and its outputs is exhibited. More recently, ANN approaches have incorporated factors other than earthquake magnitude in modelling [17], [18]. They have also been used to forecast tsunami intensity in real time with inputs obtained after the earthquake event [16]. The ensuing section presents the three modelling techniques employed in this work.

2 Modelling Techniques

The data used for the modelling had been compiled by Gusiakov [14] and covers the period from 2000 BC to 2007 AD, containing 2275 historical events. The validity (v) of the tsunami events is mapped to integers ranging from 4 (definite tsunami) to 0 (false entry). There are 776 definite tsunami events and 152 events with zero validity. This database is genuinely global in scope and characterized by parametric data that can be used for data analysis; it is also very similar to the other global database maintained by the National Ocean and Atmospheric Association [19].

2.1 Artificial Nural Network

Artificial neural networks have been used in various civil engineering problems such as predicting properties of concrete [20], buckling load of cracked columns [21], and also for construction bid decisions [22].

In this work, feed-forward ANNs with sigmoid hidden neurons and a linear output neuron were used to explore patterns in earthquake magnitude and resulting tsunami intensity. MATLAB [23] software was used to implement the neural networks, which were trained using the Levenberg-Marquardt back propagation algorithm [24]. One hidden layer with 10 neurons was found by trial and error to be the optimum. The training set contained 75% of the data, while the validation set (20% of the data) was used to measure network generalization, and to halt training when generalization stopped improving, as indicated by an increase in the mean square error (MSE) of the validation samples. The last 5% of the data provided an independent test of the network's generalization. The performance of the various ANN models is evaluated using regression analysis between network outputs and targets for all the data.

As indicated in Table 1, a range of ANN models (Rows 1 to 11) were tried, having various inputs and their combinations. The inputs used were earthquake moment magnitude (Mw), focal depth to the earthquake event (Depth), distance to the nearest coast (Dist) and tsunami efficiency, captured by TE or Rn, which stands for Gusiakov's regions [10] in a qualitative way, with the numeric inputs 3, 2 and 1 representing the red, green and blue regions respectively. The single output was tsunami intensity, either in raw or transformed state. The number of data sets used for each model is also given.

An ANN model does not give any explanation about its output and acts as a black box, thus necessitating sensitivity analyses [20]. ANFIS is a later development of ANNs that provides some rationality about its modelling process through changes in the shapes of membership functions (MFs) [26], [27].

2.2 Adaptive Network based Fuzzy Interence System

Numerous attempts have been taken to address complex problems in civil engineering using ANFIS, e.g. sediment transport [29], bridge risk assessment [30], rainfall-runoff modeling [31], and design of reinforced concrete beams [32].

In this work, an ANFIS model was created to explore the effects of earthquake magnitude (Mw) and focal depth (D) on tsunami intensity, transformed as two to the power I (Row 12 in Table 1). It is based on a zero order Sugeno-type fuzzy inference system, i.e. with constant output MFs. Preliminary studies indicated that Gaussian membership functions would yield the lowest mean square error (MSE), with 2 and 3 MFs for the inputs Mw and Depth respectively. The data set was divided into two sets, with 75% of data for training (as for the ANN exercises) and 25% of data for testing. During the learn-

ing process, ANFIS uses the training data set to adjust membership function parameters and determine the consequent parameters. The testing data provides an independent check on the ANFIS models.

2.3 Multiple Regression

After modelling tsunami intensity with ANN and ANFIS, conventional multiple linear regression analyses were performed for the 2^I versus Mw and Depth model. Several regression models were tried and the best selected (Row 13 in Table 1). Only 75% of the data was used to fit the model, as for training the ANN and ANFIS models, and the balance for testing. The regression analysis was carried out using Minitab14 software [33].

Finally, since there is a lot of scatter in the relationship between I and Mw, it was decided to use a simple relationship between I and Mw alone, where I is treated as a linear function of Mw, but to make it two valued, corresponding to the upper and lower bounds of the relationship.

3 Results and Discussion

Table 1 summarizes the results. Three indicators are used to evaluate the models: the correlation coefficient (R) between the model outputs and target recorded values, and mean square error (MSE) reflect the scatter in the model, while the slope of the best fit line between model outputs and targets reflects the degree to which the model has captured the trend.

Row 1 is the base case and is represented by Figure 1(a). There are 351 data points here (many of them overlapping); these are records from v = 1 to 4 that have I and Mw values reported. In Row 3, we have decided to focus only on events with the highest degree of validity, i.e. v = 4 [14]. This has reduced the number of data sets available to 277. (Note that although there are 776 events with v = 4, only 277 of them have I and Mw values reported). In Row 4, only data with I > 0 was used, and this has resulted in only 129 samples being available. The reason for this selection is that significant wave heights are represented only when I > 0. As per Eqn (1), the H_av corresponding to I = 0 is 0.71 m. This strategy results in a very good improvement in the MSE, which has reduced from 2.39 in Row 3 to 0.56 in Row 4. It should be noted that such grouping of data should normally be done for input as opposed to output data. However, we have used this approach to demarcate the output I values because there is only a single output, whereas we introduce various other inputs in combination with Mw. At any rate, from this row below, given that only data for I > 0 is used, we can say that the modelling represents higher end estimates for I.

From Row 5 onwards the output is a transformed version of I, namely 2^I, which is a sort of alias for the wave height – see Eqn (1). Row 5 is represented by Figure 1(b), with 129 data points (once again, many of them overlapping). We see a dramatic improvement in the R-value after this transformation. Although there is an increase in MSE compared to Row 4, the units of MSE would be different and hence cannot be compared across this transformation. In Row 6, the essentially qualitative input Rn is replaced with the quantitative one TE. It is seen subsequently that any regional effect (whether through Rn or TE) is not significant. In fact, although Gusiakov's numerical modelling gave clear boundaries between the three regions as stated before, a plot of I versus Mw for the actual raw data does not result in the three regions being demarcated at all

TABLE I. Model inputs and outputs

Row	Inputs	Output	Data sets	Slope	R	MSE	Remarks
1	M_w	I	351	0.36	0.576	2.87	**ANN ↓**
2	M_w, Rn	I	339	0.40	0.639	2.51	
3	M_w, Rn	I	277	0.45	0.656	2.39	v = 4 data ↓
4	M_w, Rn	I	129	0.49	0.678	0.56	I > 0 data ↓
5	M_w, Rn	2^I	129	0.71	0.846	6.40	
6	M_w, TE	2^I	129	0.70	0.859	6.40	
7	M_w, TE, Depth	2^I	126	0.67	0.836	6.18	
8	M_w, TE, Depth, Dist	2^I	113	0.72	0.856	6.37	
9	M_w, Depth, Dist	2^I	113	0.74	0.855	6.21	
10	M_w, Depth	2^I	126	0.74	0.861	5.93	
11	M_w	2^I	126	0.77	0.828	6.95	**ANN ↑**
12	M_w, Depth	2^I	126	0.71	0.828	6.72	**ANFIS**
13	M_w, Depth	2^I	126	0.69	0.812	7.30	**MR**

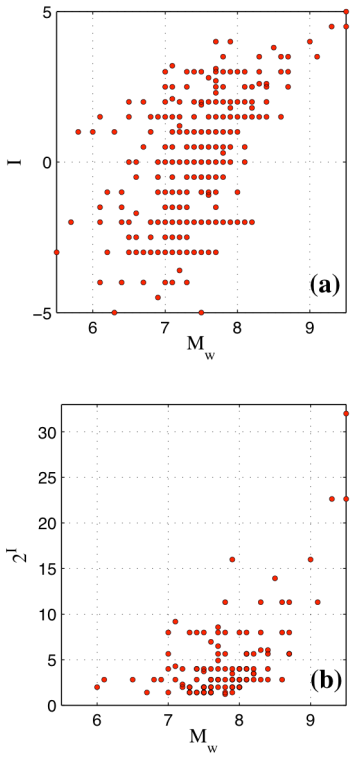

Fig. 1. Data points for ANN models; corresponding to (a) Row 1 in Table 1(the base case, showing large scatter); and (b) Row 5 in Table 1 (showing much less scatter and better trend, after data selection and transformation)

[10,14,34]. From Rows 6 to 11, focal depth and distance to shore are also added to the model, but only depth is retained at Row 10, which represents the best ANN model.

Row 12 gives the ANFIS results. The ANFIS results show slightly inferior performance compared to the ANN model in Row 10. However, as seen in Figure 2, the change in the membership functions before and after training is very informative. The line "mw1" is the support for Mw being "low" with respect to increased tsunami intensity, whereas the line "mw2" is the support for Mw being "high". After training, the "mw1" line shows that an Mw value of even 7 has a support close to unity of being "low"; while the "mw2" line shows that the support for Mw being "high" increases significantly above zero only after a value of 8. This means that Mw values of even up to 7 are unlikely to cause tsunamis, which are likely to be significant only when Mw is greater than 8.

Row 13 in Table 1 gives the MR results, which are only marginally inferior to both the ANN and ANFIS models. The advantage with MR is however its portability – i.e. an equation is readily available – and formality, with respect to determining the statistical significance of the model and its parameters. The best fitted multiple linear regression model is:

$$2^{I} = 33.9 - 4.85\,Mw + 0.0078\,D + 0.00293\exp(Mw) \qquad (2)$$

where D is in km.

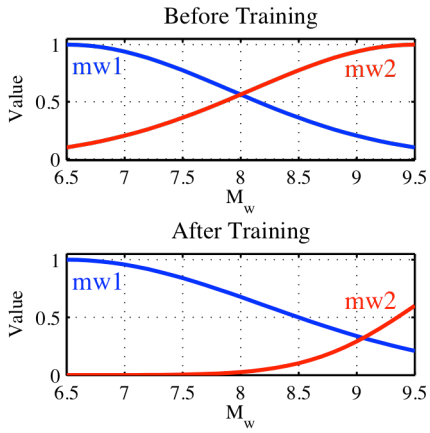

Fig. 2. ANFIS membership functions for M_w; with "mw1" corresponding to "low" and "mw2" to "high", before training (top) and after training (bottom), showing marked variation.

The t-statistic for each predictor was computed and these indicated that all the parameters except focal depth (D) are significantly different from zero. Although the contribution from depth (D) is not statistically significant even at a 10% level, it was kept in the model since the ANN and ANFIS models were mildly sensitive to it too [34]. While tsunami intensity should generally decrease with increasing focal depth, it should also be noted that 65% of the D values were below 35 km; such data points may have dominated the parameters, resulting in I showing an increase with D, as found by Gica et al. [13] in that range too; they indicate that the effect of focal depth is not very significant, which also agrees with our findings.

Looking at the form of Eqn (2), it can be considered primarily as a linear relationship between 2^I and exp(Mw). If a logarithmic version of this is considered, it yields a form that is quite similar to the linear relationship between I and Mw advocated by other authors [2]. However, since the exp(Mw) term would tend to over-predict I at higher Mw values and vice versa, the (33.9 – 4.85 Mw) component of the equation serves as a corrective for this tendency. The (0.0078 D) term adds very little to the result. It should be noted that all these models have been derived for Mw values ranging from 6.5 to 9.5 and D values ranging from 1 km to 83 km; hence they should only be used within those ranges.

Figures 3 (a), (b), and (c) give a comparative assessment of the ANN, ANFIS and MR models respectively. The dashed lines denote points where the outputs and targets would be equal, and the solid lines give the best-fit lines between model outputs and targets. All three models tend to over-predict at low I values and under-predict at high ones. Although the ANN model has slope and R-value closest to unity (and is hence the best model), the differences between the models are not that great; and each approach has its advantages, as described above.

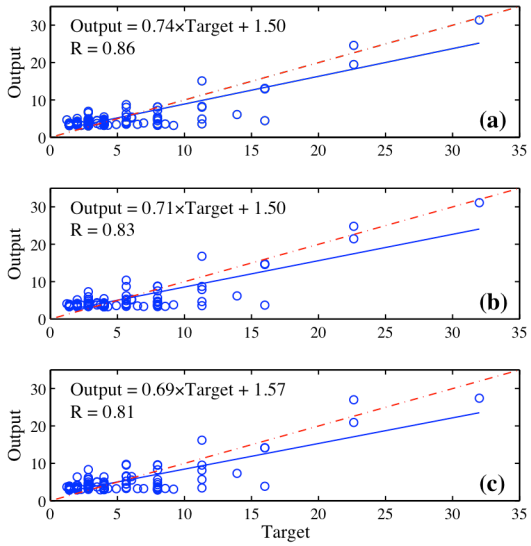

Fig. 3. Comparison of predictions from the best models out of (a) ANN; (b) ANFIS; and (c) MR models

Finally, Figure 4 shows a different (and simple) approach for deriving a two-valued estimate for I from Mw alone, once again using the well-established linear relationship, but in a different way. The upper and lower linear regression lines are lines of best fit through the uppermost and lowermost I values for Mw values ranging from 7 to 9.5. The fitted data points are at the top and bottom extremities of the v = 4 data only in Figure 1(a). The modified lines (for which equations are given) are obtained by making parallel shifts until the lines pass through the two I values available for Mw = 9.5. It should be noted that the gap between the two lines closes quickly with the increase in Mw.

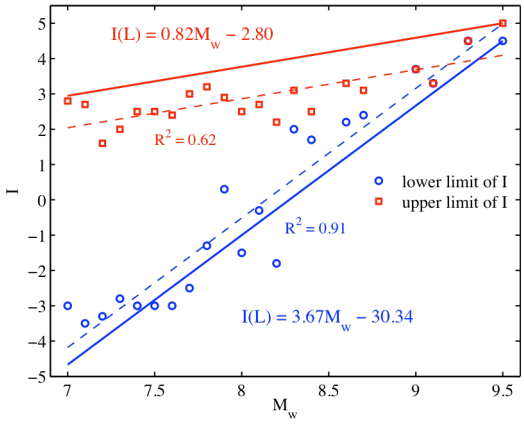

Fig. 4. Two valued estimates for I from M_w

Table 2 gives some actual Mw, D and I values and compares these actual I values with the predictions from the models in this paper. For the first two and next three rows the data was directly obtained from Gusiakov [14] and the Historical Tsunami Database for the World Ocean [35], respectively. Since the latter did not have data for the last three rows, the data was obtained from the National Ocean and Atmospheric Association [19] database, from which the I value had to be calculated as per Eqn (1), using the run-up for the nearest coast. The first two data rows represent data points that are already included in the modelling. The last five data rows represent data points that have not been used in the models and are hence a good test of the model.

All of the data points have fairly high Mw values. The I values of the last three data rows are not well predicted by the model, because they are low values. This is to be expected because the modelling was focused on combinations that gave I values larger than zero – see Figure 1(b). The modelling works

TABLE II. PERFORMANCE OF MODELS IN GENERATING I VALUES, IN BOTH FITTING AND PREDICTING MODE

		Actual Values			Predicted I				
								Linear	
Date	Place	Mw	D (km)	I	ANN	ANFIS	MR	UB	LB
2004.12.26	Indonesia	9.3	10	4.5	4.5	4.6	4.4	4.8	3.8
2005.03.28	Indonesia	8.6	30	1.5	2.8	2.7	3.1	4.2	1.2
2010.02.27	Chile	8.8	35	3.0	3.2	3.4	3.4	4.4	1.9
2011.03.11	Japan	9.0	24	4.1	4.3	4.1	4.0	4.6	2.6
2011.07.06	New Zealand	7.6	18	**0.6**	2.1	1.9	1.6	3.4	-2.6
2012.04.11	Indonesia	8.6	23	**0.6**	2.8	2.9	3.0	4.2	1.2
2012.04.11	Indonesia	8.2	23	**-1.6**	1.7	2.1	2.3	3.9	-0.3

very well especially for such combinations reflected in the first four data rows, the first two having been fitted by the models but the next two actually predicted.

Although the I values in the last three data rows are not well predicted, the actual I value for the New Zealand tsunami is within the upper and lower bounds of the linear model shown in Figure 4. However, for the two Indonesian tsunamis in 2012, the actual I values are below even the lower bound of the linear model. Here too, the I value of the first tsunami (Mw = 8.6) is not too much below the lower bound; the second tsunami (Mw = 8.2) was an aftershock and perhaps not typical. We could argue that the linear model of Figure 4 does in fact help somewhat to explain the variability in tsunami heights that can be expected even from earthquakes with Mw values greater than 8. However, in future, more work needs to be done to model how high Mw values sometimes result in low I values, perhaps by taking into account the type of tsunamigenic earthquake [11].

4 Conclusions

Earthquake magnitude (Mw) is the most significant parameter among others examined (i.e. focal depth, tsunami efficiency, and distance to the nearest shore), which affects the resulting tsunami intensity (I). Transforming the I values to 2^I (which is a sort of alias for wave height) yields better correlations.

The performance of ANN is better when compared with the other two modelling schemes, i.e. ANFIS and multiple regressions. However, the changes in ANFIS membership functions give us some genuine domain knowledge. The ANFIS modelling shows that it is only when Mw values are greater than around 8 that significant tsunamis are caused; whereas Mw values of even up to 7 are unlikely to cause tsunamis.

There is a large scatter of I versus Mw, justifying a two-valued prediction scheme, but this scatter reduces significantly with the increase of Mw. Although the two-valued linear models helps to predict the largest and smallest I values that can be expected, more work needs to be done to model how high Mw values sometimes result in low I values.

Acknowledgment

The authors acknowledge Dr. V. K. Gusiakov for access to his database of tsunami events. This work was supported by the University of Moratuwa Senate Research Committee under Grant No. 313.

References

[1] K. Iida, "Magnitude and energy of earthquakes accompanied by tsunamis, and tsunami energy," Journal of Earth Sciences, vol. 6(2), pp. 101-112, 1958.

[2] L. B. Chubarov and V. K. Gusiakov, "Tsunamis and earthquake mechanism in the Island arc region " Science of Tsunami Hazard, vol. 3(1), pp. 3-21, 1985.

[3] M. E. Blackford, "Use of relationships between moment magnitude and water level measurement station amplitudes by the tsunami warning system to forecast tsunamis in the far field" Proc. 29th Joint Meeting UJNR Panel on Wind and Seismic Effects Tsukuba, Japan, pp. 419-422, 1997.

[4] E. A. Okal, "Seismic parameters controlling far field tsunami amplitude: A review," Natural Hazards, vol. 1, pp. 67-96, 1988.

[5] E. L. Geist, " Complex earthquake rupture and local tsunamis," Journal of Geophysical Research B: Solid Earth, vol. 107(5), 2002.

[6] E. L. Geist, S. L. Bilek, D. Arcas and V. V. Titov, "Differences in tsunami generation between the December 26, 2004 and March 28, 2005 Sumatra earthquakes," Earth Planets Space, vol. 58, pp. 185-193, 2006.

[7] K. Abe, "Estimate of tsunami run-up heights from earthquake magnitudes, in Tsunami: Progress in Prediction, Disaster Prevention and Warning," Adv. Nat. Technol. Hazards Res., vol. 4, pp. 21– 35, 1995.

[8] E. Gica, M. H. Teng, P. L. -F. Liu, V. Titovand, and H. Zhou, "Sensitivity analysis of source parameters for earthquake generated distant tsunamis," Journal of Waterway, Port Coastal and Ocean Engineering, vol. 133(6), pp. 429-441, 2007.

[9] D. L. Wells and K. J. Coppersmith, "New empirical relationships among magnitude, rupture length, rupture width, rupture area, and surface displacement," Bulletin of the Seismological Society of America, vol. 84(4), pp. 974-1002, 1994.

[10] V. K. Gusiakov, "Tsunami generation potential of different tsunamigenic regions in the Pacific," Marine Geology, vol. 215, pp. 3-9, 2005.

[11] V. K. Gusiakov, "Relationship of tsunami intensity to source earthquake magnitude," Pure and Applied Geophysics, vol. 168, pp. 2033-2041, 2011.

[12] T. Hanks, and H. Kanamori, H. "A moment magnitude scale," Journal of Geophysics, vol. 84, pp. 2348-2350, 1979.

[13] S. L. Soloviev, "Recurrence of earthquakes and tsunamis in the Pacific Ocean," In: Volny Tsunami (Tsunami Waves), Trudy Sakh CNII, vol. 29, pp. 7-47, 1972.

[14] V. K. Gusiakov, "Tsunami history – recorded," The Sea, vol. 15, pp. 23-51, 2009.

[15] N. Ambraseys, and C. Synolakis, "Tsunami catalogues for the Eastern Mediterranean, revisited," Journal of Earthquake Engineering, vol. 14(3), pp. 309-330, 2010.

[16] S. Namekar, Y. Yamazaki, and K. F. Cheung, "Neural network for tsunami runup forecast," Geophysical Research Letters, vol. 36(8), 2009.

[17] M. Srivichai, S. Supharatid, and F. Imamura, "Developing of forecasted tsunami database along Thailand Andaman coastline," Proc. Asia Oceania Geosciences Society 3rd Annual Meeting, pp. 138-141, 2006.

[18] M. Romano, S. Y. Liong, S. Vu, M. T. Zemskyy, P. Doan, C. D. Dao and M. H. Tkalich, "Artificial neural network for tsunami forecasting," Journal of Asian Earth Sciences, vol. 36, pp. 29-37, 2009.

[19] National Ocean and Atmospheric Association (2012). http://www.ngdc.noaa.gov/nndc/struts/form?t=101650&s=70&d=7.

[20] W. P. S. Dias and S. P. Pooliyadda, "Neural networks for predicting properties of concrete with admixtures," Construction and Building Materials, vol. 15, pp. 371-379, 2001.

[21] M. Bilgehan, M. A. Gürel, R. K. Pekgökgöz, and M. Kısa, "Buckling load estimation of cracked columns using artificial neural network modelling technique," Journal of Civil Engineering and Management, vol. 18(4), pp. 568-579, 2012.

[22] W. P. S. Dias and R. L. D. Weerasinghe, "Artificial neural networks for construction bid decisions," Civil Engineering Systems 13.3 (1996): 239-253.

[23] MATLAB, Version 2008a (2008) The MathWorks, Inc. Natick, MA, USA.

[24] D. Marquardt, "An algorithm for least-squares estimation of nonlinear parameters," SIAM Journal on Applied Mathematics, vol. 11(2), pp. 431–441, 1963.

[25] W. C. Carpenter, and J.-F. Barthelemy, "Common misconceptions about neural networks as approximators," Journal of Computing in Civil Engineering, vol. 8(3), pp. 345-358, 1994.

[26] I. Flood and N. Kartam, "Neural networks in civil engineering - I: Principles and understanding" Journal of Computing in Civil Engineering, vol. 8(2), pp. 132-148, 1994.

[27] J.-S. R. Jang, "ANFIS: Adaptive network based fuzzy inference system," IEEE Transactions on System, Man and Cybernetics, vol. 23(3), pp. 665-684, 1993.

[28] J.-S. R. Jang, and C.-T Sun "Neuro-fuzzy modelling and control," Proc. of the IEEE, vol. 83(3), pp. 378-405, 1995.

[29] H. M. Azamathulla, A. A. Ghani, and S. Y. Fei, "ANFIS-based approach for predicting sediment transport in clean sewer," Applied Soft Computing, vol. 12(3), pp. 1227-1230, 2012.

[30] A. Tarighat, "Model based damage detection of concrete bridge deck using Aadaptive neuro-fuzzy inference system," international journal of civil engineering, vol. 11(3A), pp. 170-181, 2013.

[31] M. Shoaib, A. Y. Shamseldin, B. W. Melville and M. M. Khan "Hybrid Wavelet Neuro-Fuzzy Approach for Rainfall-Runoff modelling," Journal of Computing in Civil Engineering, vol. 30, 04014125, 2014.

[32] J. P. Yeh and R. P. Yang, R. P. "Application of the Adaptive Neuro-Fuzzy Inference System for Optimal Design of Reinforced Concrete Beams" Journal of Intelligent Learning Systems and Applications, vol. 6(04), pp. 162-175, 2014.

[33] Minitab, Version 14 (2003) State College, PA, USA.

[34] M. A. N. Dewapriya, "Exploring patterns in historic earthquake and tsunami data," MSc thesis, University of Moratuwa, December 2009.

[35] Historical Tsunami Database for the World Ocean (2012) http://tsun.sscc.ru/nh/tsunami.php